Contactless measurements of microwave-induced resistance oscillations in a ZnO/MgZnO heterojunction

A. V. Shchepetilnikov,[1,*] A. R. Khisameeva,[1,2] Yu. A. Nefyodov,[1] and I. V. Kukushkin[1]
[1]*Institute of Solid State Physics RAS, 142432 Chernogolovka, Moscow district, Russia*
[2]*Moscow Institute of Physics and Technology, Dolgoprudny 141700, Russia*

(Received 14 August 2019; revised manuscript received 28 August 2019; published 17 September 2019)

The high-frequency conductivity of the two dimensional electron system formed at a ZnO/MgZnO heterojunction was investigated in the 4–18 GHz frequency range at high Landau level fillings and in the regime of both integer quantum Hall effect. The conductivity was probed by measuring the transmission of the broadband coplanar waveguide deposited on the sample surface. At low magnetic fields in case the sample was additionally subjected to the exciting radiation of the 60–140 GHz frequencies, the high-frequency conductivity exhibited well developed microwave-induced oscillations. Remarkably, these oscillations were detected in the whole range of probe frequencies studied—up to 18 GHz—in contrast to GaAs/AlGaAs heterostructures, where microwave-induced oscillations were reported to smear out at probe frequencies around 1 GHz. Furthermore, for each exciting frequency the phase and the period of the microwave-induced oscillations revealed no dependence on the probe frequency and coincided with the period and phase of the microwave-induced resistance oscillations studied independently by dc transport measurements in the same sample. The characteristic probe frequency at which the oscillations start to degrade corresponds to the characteristic scattering time in the region between quantum scattering rates deduced from the cyclotron resonance linewidth and that extracted from the magnetic field dependence of the microwave-induced resistance oscillations.

DOI: 10.1103/PhysRevB.100.125425

I. INTRODUCTION

Oscillations of the longitudinal magnetoresistance induced by microwave radiation in a high quality two dimensional electron system represent one of the most significant nonequilibrium transport phenomena in semiconductor physics. Since its discovery [1–3] extensive research efforts reviewed in Ref. [4] have been dedicated towards exploring its major physical properties. The origin of this phenomenon still remains a puzzle and is a subject of discussion, as several experimental aspects are still not accounted for. The complete immunity of the oscillations amplitude to the helicity of the incident microwave radiation in semiconductor heterostructures [5,6] and renormalization of the mass governing the oscillations period caused by $e-e$ interactions [7–10] may be mentioned as bright examples. Thus the ongoing research in the field remains of exceptional interest.

The conventional experiments exploring the microwave-induced resistance oscillations (MIRO) imply the direct current (dc) magnetotransport measurements in high quality GaAs/AlGaAs quantum wells under microwave irradiation. For that purpose, the samples are prepared in a Hall bar [1,3], Van der Pauw [11], or Corbino ring geometry [12,13] with annealed Ohmic contacts. Yet a number of high frequency techniques including capacitative approach [14,15] and analysis of the coplanar waveguide (CPW) attenuation [16] have been recently demonstrated to be capable of contactless MIRO detection. While the possibility to observe MIRO without forming Ohmic contacts to the 2DES is crucial to the understanding of MIRO nature by itself, the implementation of the aforementioned techniques boasts of another important advantage. The dynamics of MIRO may be studied in detail by analyzing major MIRO properties in a wide frequency range of the probe signal. In our experiments we were able to extend the probe frequency range by the order of magnitude from $f \sim 1$ GHz reported earlier [16] up to 18 GHz.

Till now contactless detection of MIRO was limited by the case of conventional GaAs/AlGaAs heterostructures, yet application of these high-frequency techniques to the study of MIRO in new materials is of great importance, as some of the most remarkable MIRO features were reported to be material dependent. For instance, the MIRO amplitude was reported to be sensitive to the helicity of the microwave radiation in the 2DES at the surface of liquid helium [17] in contrast to results obtained in semiconductor heterostructures [5,6]. In the present paper we report on the studies of microwave-induced oscillations of the high-frequency conductance probed by the transmission of the broadband coplanar waveguide deposited on top of a ZnO/MgZnO heterojunction—a material system with unique properties essentially distinct from that of the traditional GaAs/AlGaAs quantum wells. For instance, the effective mass of 2D electrons in a ZnO-based 2D electron system (2DES) was reported to be $m = 0.33m_0$—the value much larger than in GaAs [10,18,19]; here m_0 is a free electron mass. Such heavy mass leads to the enhancement of the e-e correlations [20,21] that affect even such basic properties of MIRO as the oscillation period [8–10].

*shchepetilnikov@issp.ac.ru

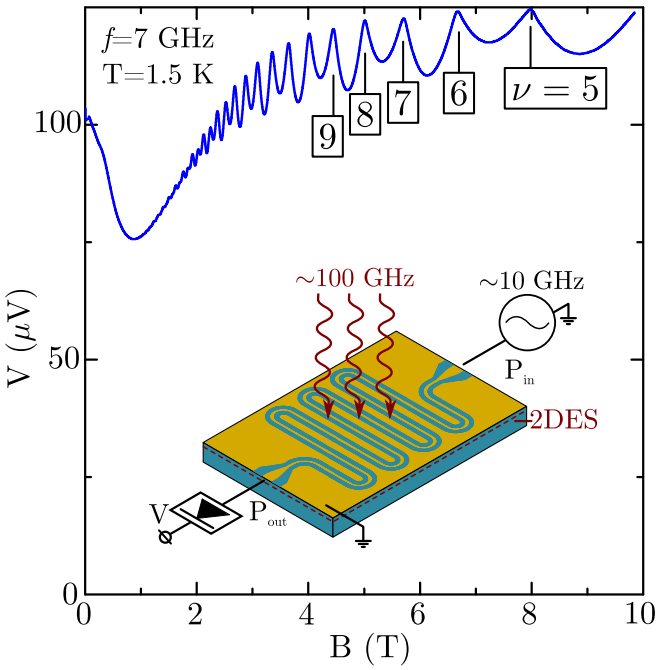

FIG. 1. Typical dc voltage measured at the Shottky diode detector output vs the magnetic field. The probe frequency was fixed at 7 GHz and the temperature was equal to 1.5 K. The positions of several Shubnikov–de Haas minima are indicated. In the inset the experimental setup is schematically illustrated.

II. SAMPLES

The sample under study represented a slab of the ZnO/MgZnO heterojunction with a high quality 2DES formed at the interface due to the difference in the inner electric polarization of the ZnO and MgZnO material [22–24]. The sample was immersed into the liquid helium in the 1 K pot of the cryostat, so that experiments were carried out at the temperature of 1.5 K. The electron density equaled $n = 9.6 \times 10^{11}$ cm^{-2} and the low temperature dc mobility was 3×10^4 cm^2/V s. Although the mobility of the sample under study was several orders of magnitude lower than that deemed necessary for the observation of MIRO in the conventional GaAs/AlGaAs quantum wells, remarkably, MIRO were clearly resolved in the dc magnetotransport experiments [10,25]. This unique property of nonequilibrium magnetotransport in ZnO-based 2DES is yet to be understood.

III. EXPERIMENTAL METHOD

The sample surface was passivated with a 1 μm thick layer of photoresist, as metallic pads deposited directly on the sample surface act as Ohmic contacts to the 2DES [26]. A meander CPW line with the slot width of 30 μm was formed on top of the photoresist as schematically illustrated in Fig. 1. The probe signal produced by the microwave generator was applied to the central strip, while the large metal areas on either side of the strip were grounded. In the slot regions propagating wave generates high-frequency electric field that effectively interacts with the 2D electrons; as a result, the energy of the wave is dissipated. The power P of the transmitted wave is rectified by a room-temperature Schottky diode detector to yield a dc voltage V proportional to the value of P. The frequency bandwidth of the detector imposed the 18 GHz limitation on the highest probe frequency used in our experiments.

Under ideal conditions one might express the micorwave power transmitted through a waveguide as [27]

$$\mathrm{P} = \mathrm{P}_i \exp(-\alpha\sigma_{xx}), \tag{1}$$

where P_i is the initial power of the wave before entering CPW, σ_{xx} is the real part of the 2DES longitudinal conductivity, and α is a coefficient defined mainly by the geometrical dimensions of the CPW and dielectric properties of the surroundings. Thus the high-frequency conductivity of the 2DES may be experimentally accessed by measuring the attenuation of the CPW line. Typical voltage acquired in a wide range of magnetic fields is presented in Fig. 1 for the probe frequency of $f = 7$ GHz. The power of the probe microwave radiation was chosen so that the heating of the 2DES due to the radiation absorption was negligible and the detector was operating in the quadrature regime. In the region of high magnetic fields the Shubnikov–de Haas oscillations of the high frequency conductivity are clearly resolved, indicating that a substantial part of the probe radiation is, indeed, absorbed by 2DES. Note that parasitic losses are inevitably present in the experimental setup and may originate from dissipation in coaxial lines, connectors, and microstrip-to-coaxial transitions and also from reflection in those transitions and at CPW ends. Yet these losses are not associated with the 2DES absorption and, thus, do not depend on the magnetic field and only alter the prefactor in Eq. (1).

For the contactless studies of MIRO the sample was additionally subjected to the exciting radiation in the frequency range of F = 60–140 GHz delivered to the sample through an oversized rectangular waveguide. Frequency multipliers coupled with a microwave generator were used as the source of exciting radiation. This radiation modifies the 2DES conductivity by a small amount $\delta\sigma_{xx}$, resulting in the variation of the transmitted power δP. Note that according to Eq. (1) the value δP/P is linearly proportional to $\delta\sigma_{xx}$. Typical dependence of the transmitted power on the magnetic field with and without exciting radiation is presented in Fig. 2(a) for the probe and exciting frequencies of $f = 7$ GHz and F = 140 GHz, respectively. As can be clearly seen, the microwave radiation does induce the oscillations of the high-frequency conductivity.

In order to increase signal-to-noise ratio the standard lock-in scheme was adopted. The exciting microwave radiation was amplitude modulated at the frequency of ~30 Hz and the lock-in amplifier synchronized at that exact frequency took a signal from the output of the Shottky-diode detector and, in fact, measured the variation of the transmitted power δP due to the absorption of the excited radiation. This approach is illustrated in panel (b) of Fig. 2, where the variation δP induced by the exciting radiation of the 140 GHz frequency is presented. The microwave-induced oscillations of the transmitted power and, hence, of the high-frequency conductivity are unambiguously resolved. The oscillations observed in δP and dc transport

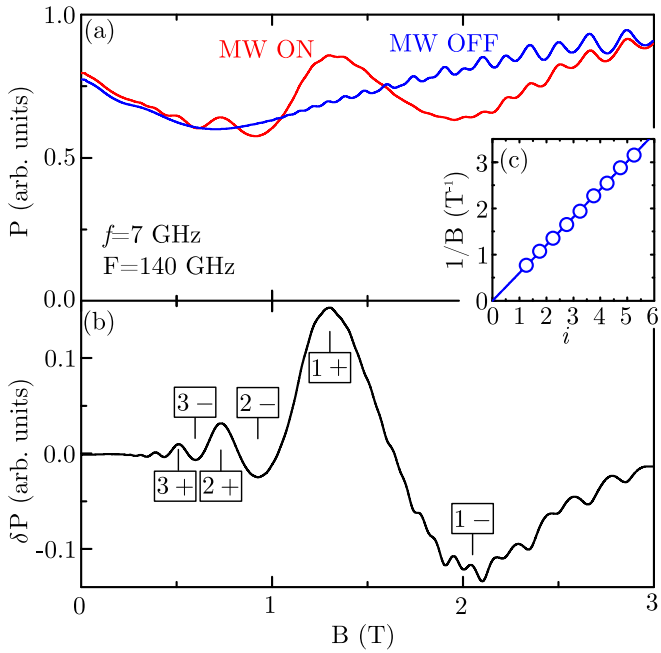

FIG. 2. (a) Typical dependence of the transmitted power on the magnetic field in the presence of exciting radiation (red line) and without any exciting radiation (blue line). The frequencies of the probe and exciting radiation were fixed at 7 and 140 GHz; temperature was 1.5 K. (b) The variation of the transmitted power induced by the exciting radiation measured with the aid of lock-in technique under the same conditions as in panel (a). The positions of the first several oscillations are indicated. (c) The dependence of the inverse magnetic field positions of the oscillations on $i = n - 1/4$ for minima and $i = n + 1/4$ for maxima. The solid line represents the fit with the equation $i = 2\pi \mathrm{F} m^*/eB$.

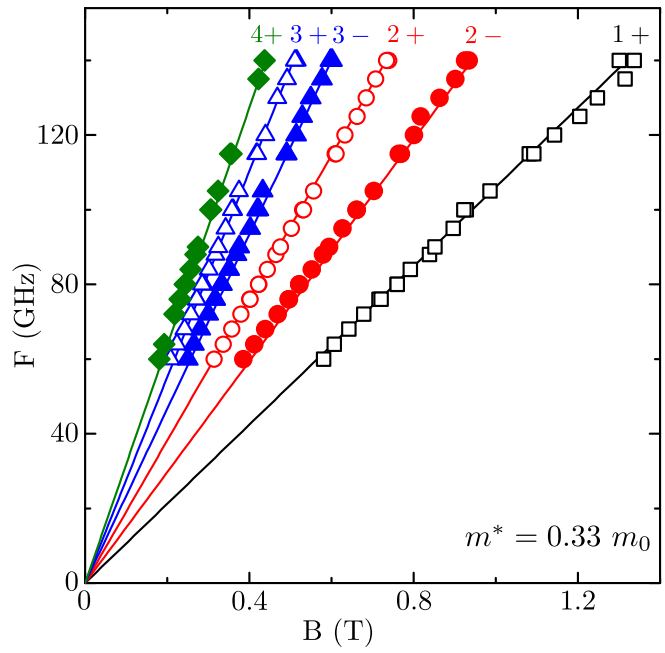

FIG. 3. Magnetic field dispersion of the microwave-induced oscillations of the transmitted power through the CPW line. The correspondent oscillations number is denoted near each data set. The lines represent fits according to $\mathrm{F} = (n + 1/4)eB/2\pi m^*$ for the position of nth maxima and $\mathrm{F} = (n - 1/4)eB/2\pi m^*$ for the nth minima. The fits were performed with a single free parameter—effective electron mass $m^* = 0.33 m_0$. The probe frequency was fixed at $f = 7$ GHz.

MIRO are clearly of the same physical origin, as the major oscillation properties will be demonstrated to be alike.

IV. RESULTS AND DISCUSSION

In the MIRO regime the oscillatory part of the conductivity was reported [12] to follow the equation

$$\delta \mathrm{P} \sim -\delta\sigma_{xx} \sim \sin(2\pi\varepsilon + \varphi). \tag{2}$$

Here $\varepsilon = \omega/\omega_c$ represents the ratio between the microwave and cyclotron frequencies and φ is the phase of these oscillations. Typically, φ equals zero, resulting in the magnetic field position of the oscillations extrema correspondent to $\varepsilon = n \pm 1/4$, where $n = 1, 2, 3 \ldots$. To test the value of φ we plot the values of the inverse magnetic field positions of the nth oscillation minimum and maximum vs $\varepsilon = n - 1/4$ and $\varepsilon = n + 1/4$, respectively. The minima of the first oscillation is usually omitted during the analysis as its position is obscured by the overlapping Shubnikov–de Haas oscillations. The resulting dependence turned out to be linear starting from the point of origin for every exciting frequency studied; thus the assumed zero value of φ is correct. This experimental finding is illustrated in Fig. 2(c), where the correspondent dependence for $F = 140$ GHz and $f = 7$ GHz is demonstrated. Zero phase of the oscillation coincides with the dc transport MIRO phase obtained on the sample from the exact same wafer in our previous work [10].

The position of the oscillations extrema is defined by the commensurability between the frequency of the exciting microwave radiation and the cyclotron frequency. The experimental dependence of the magnetic field positions of the first several oscillations' minima and maxima on the exciting microwave frequency is demonstrated in Fig. 3 for the probe frequency $f = 7$ GHz. Solid lines in the same figure represent the fits with $\mathrm{F} = (n + 1/4)eB/2\pi m^*$ for the position of nth maxima and $\mathrm{F} = (n - 1/4)eB/2\pi m^*$ for the correspondent minima in full accordance with Eq. (2). The fitting was performed with a sole free parameter—the effective mass m^* of the electron—to yield the value $m^* = 0.33 m_0$. Exactly the same mass was extracted from the period of MIRO in dc conductivity in Ref. [10]. One might conclude that the observed oscillations of the transmitted power are, in fact, directly related to MIRO. The insignificance of the contacts for the observation of MIRO established here for the ZnO-based 2DES is important for the understanding of the MIRO physical nature.

The direct relation between the MIRO detected in dc transport and the observed oscillations of the transmitted power has another important implication, as the MIRO dynamics may be explored by varying the frequency of probe radiation propagating through the CPW line with the exciting frequency kept constant. This process is illustrated in Fig. 4, on the left panel of which the variation of the transmitted power induced by the exciting radiation of 75.9 GHz frequency is

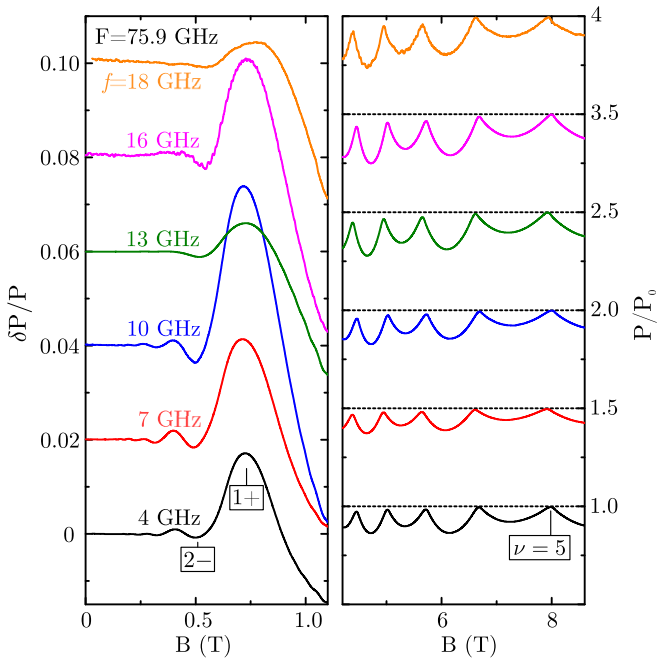

FIG. 4. On the left panel the variation of the transmitted power induced by the exciting radiation of 75.9 GHz frequency is presented for a set of probe frequencies. The traces are offset for clarity. On the right panel the transmitted power is demonstrated in the regime of high magnetic field where the Shubnikov–de Haas oscillations are fully developed. The power value is normalized by the amount of the transmitted power at the exact filling factor of $\nu = 5$. The traces are offset for clarity.

presented for a set of probe frequencies. On the right panel of the same figure the transmitted power at the exact same probe frequencies is demonstrated in high magnetic fields where well-developed Shubnikov–de Haas oscillations have already emerged. The value of P was normalized by the amount of the transmitted power at the exact filling factor of $\nu = 5$. Note that at well-developed minima of Shubnikov–de Haas oscillations $\sigma_{xx} = 0$ and according to Eq. (1) the absorption associated solely with 2DES should equal zero. All traces are shifted for clarity with the correspondent value of f indicated nearby. The increase of the probe frequency does not result in any detectable shift of the microwave-induced oscillations' extrema, indicating that the phase of the oscillation and the effective mass governing the MIRO period do not change in the whole range of f studied. Yet the amplitude of these oscillations clearly depends on the probe frequency. Whereas the oscillations with large numbers n smear out for the frequencies larger than $f = 10$ GHz, the maximum correspondent to $\varepsilon = 1 + 1/4$ and the minima with $\varepsilon = 2 - 1/4$ clearly survive in the whole range of probe frequencies studied. Remarkably, the range of the probe frequencies where MIRO was observed in the present manuscript turned out to surpass that reported for GaAs-based 2DES. However, the MIRO amplitude depends on the probe frequency in a nonmonotonic way. Note that in Ref. [16] the dependence of MIRO amplitude on the value of f is clearly a mixture of the similar nonmonotonic dependence and the fast decaying function. Moreover, in the above mentioned manuscript the amplitude of Shubnikov–de Haas oscillations is nonmonotonic as well. This effect may be of an instrumental nature, as Eqs. (1) and (2) are valid only under ideal conditions, as the electric field distribution of the propagating probe signal may vary at different frequencies.

The comparison of high-frequency MIRO characteristics in ZnO- and GaAs-based 2DES is of significant interest, as these two material systems are essentially distinct. The high-frequency MIRO was probed by CPW attenuation in Ref. [16]. Quite conveniently, the experimental data is presented both in the above mentioned publication and in the present manuscript for the same base temperature of 1.5 K and for the very close values of the exciting frequency F = 80 GHz and 75.9 GHz, respectively. The absolute amplitudes of the MIRO oscillations depend on the power level of the exciting radiation and, thus, may not be directly compared, as typical power levels are not known for Ref. [16]. Yet the variation of MIRO amplitudes with the frequency may be analyzed. In GaAs the amplitude of the second oscillation decreases by the order of magnitude at the probe frequency of 1.5 GHz, whereas in ZnO-based 2DES the second oscillation clearly survives up to $f = 18$ GHz with its amplitude changed by a factor of three if compared to the data for $f = 10$ GHz. This experimental observation illustrates the key difference in the high frequency behavior of MIRO in GaAs- and ZnO-based heterostructures that is yet to be understood. Increasing probe frequency had a relatively small effect on the Shubnikov–de Haas oscillations both in GaAs- and ZnO-based 2DES as well.

We would like to highlight that the MIRO dynamics even in GaAs quantum wells remain unaccounted for; furthermore, the comprehensive theory explaining all MIRO features is still a subject of discussion. These two facts combined make it almost impossible to quantitatively describe high-frequency MIRO in the ZnO/MgZnO heterojunction reported here. However, some qualitative conclusions may be derived from the experimental data. In a typical dc experiment MIRO is observed when the 2D electron channel is subjected to the exciting microwave radiation and static electric field generated by the dc current applied to the channel. In our case the correspondent electric field is created by the probe signal wave propagating through the CPW and, thus, is essentially alternating. If the electric field changes its direction slowly, then the situation is no different from the dc case and no decay of MIRO should be observed. At higher frequencies, the response of the 2D electron system cannot keep up with the driving electric field and, thus, MIRO should start to decay. In some sense, this situation is similar to the well-known Drude model of the high-frequency conductivity. For sufficiently large exciting frequencies the characteristic probe frequency at which the actual decay becomes observable is then defined by some characteristic time $1/\tau$. In the Drude model this τ simply represents the transport scattering time; however, for the high-frequency MIRO the situation is clearly far more complicated. The transport scattering time in ZnO is about 200 times smaller than in GaAs; hence the degradation of MIRO in ZnO-based 2DES should be observed at the frequencies orders of magnitude larger than that studied here. Yet the decay is clearly detected in our experiments. The possible candidate is quantum scattering time τ_q that defines the magnetic field dependence of MIRO amplitude. Note that

the τ_q deduced from the low field behavior of the Shubnikov–de Haas oscillations usually differs from that of MIRO, as Shubnikov–de Haas oscillations are extremely sensitive to the long range density variations and, thus, represent the inhomogeneous broadening of Landau levels. In contrast the period and phase of MIRO depends rather weakly on 2D electron density, and thus MIRO τ_q is local. Taking into account typical values of MIRO τ_q in ZnO and GaAs reported in Refs. [25,28], one might calculate the correspondent frequencies of 30 GHz for ZnO and 10 GHz for GaAs. Although these values are closer to the actual probe frequencies at which MIRO decay is observed, they are still slightly higher. It is instructional to consider the τ_{CR}—the quantum scattering time extracted from the width of the cyclotron resonance (CR). The values of τ_{CR} reported for ZnO [18] and GaAs [29] yield $f = 5$ GHz and $f = 1$ GHz, respectively—values smaller than the probe frequency at which the decay is observed experimentally. Thus one might conclude that the MIRO dynamics is determined by the characteristic time in the region between the quantum scattering time deduced from the CR linewidth and the one extracted from the MIRO amplitude magnetic field dependence. Note that the MIRO is extremely sensitive to the details of the disorder that scatters electrons [30] and, even if both transport and quantum scattering rates are fixed constant in the 2DES channel, the MIRO amplitude may vary strongly from sample to sample. The possibility to observe MIRO in such essentially distinct structures with different transport and quantum scattering times as GaAs/AlGaAs quantum wells [1], ZnO/MgZnO heterojunctions [25], Ge/SiGe quantum wells [31], and 2DES on the surface of the liquid helium [32] proves this statement.

V. CONCLUSION

In conclusion, the high-frequency conductivity of ZnO-based 2DES was explored in the 4–18 GHz probe frequency range by measuring the transmission of the broadband coplanar waveguide deposited on the sample surface. At low magnetic fields in case the sample was additionally irradiated by the exciting radiation of the 60–140 GHz frequencies, the high-frequency conductivity exhibited well developed microwave-induced oscillations. These oscillations were demonstrated to be directly related to dc MIRO, as the phase and the period of these oscillations turned out to be equal. This experimental finding suggests the insignificance of Ohmic contacts for the observation of MIRO in ZnO-based 2DES. Furthermore, we were able to substantially extend the probe frequency range where microwave-induced oscillations of the high-frequency conductivity were observed, as MIRO were established to be clearly resolved at the probe frequencies up to 18 GHz in contrast to GaAs/AlGaAs heterostructures, where microwave-induced oscillations smeared out around 1 GHz [16]. Qualitative analysis of the high frequency MIRO behavior demonstrates that MIRO dynamics is defined by the characteristic time in the region between the quantum scattering time deduced from the CR linewidth and the one extracted from the magnetic field dependence of the MIRO amplitude.

ACKNOWLEDGMENTS

We acknowledge the financial support from Russian Science Foundation (Grant No. 19-72-30003). We thank Joseph Falson for the ZnO/MgZnO samples.

[1] M. A. Zudov, R. R. Du, J. A. Simmons, and J. L. Reno, Phys. Rev. B **64**, 201311(R) (2001).
[2] P. D. Ye, L. W. Engel, D. C. Tsui, J. A. Simmons, J. R. Wendt, G. A. Vawter, and J. L. Reno, Appl. Phys. Lett. **79**, 2193 (2001).
[3] R. G. Mani, J. H. Smet, K. von Klitzing, V. Narayanamurti, W. B. Johnson, and V. Umansky, Nature (London) **420**, 646 (2002).
[4] I. A. Dmitriev, A. D. Mirlin, D. G. Polyakov, and M. A. Zudov, Rev. Mod. Phys. **84**, 1709 (2012).
[5] J. H. Smet, B. Gorshunov, C. Jiang, L. Pfeiffer, K. West, V. Umansky, M. Dressel, R. Meisels, F. Kuchar, and K. von Klitzing, Phys. Rev. Lett. **95**, 116804 (2005).
[6] T. Herrmann, I. A. Dmitriev, D. A. Kozlov, M. Schneider, B. Jentzsch, Z. D. Kvon, P. Olbrich, V. V. Bel'kov, A. Bayer, D. Schuh, D. Bougeard, T. Kuczmik, M. Oltscher, D. Weiss, and S. D. Ganichev, Phys. Rev. B **94**, 081301(R) (2016).
[7] A. T. Hatke, M. A. Zudov, J. D. Watson, M. J. Manfra, L. N. Pfeiffer, and K. W. West, Phys. Rev. B **87**, 161307(R) (2013).
[8] A. V. Shchepetilnikov, D. D. Frolov, Yu. A. Nefyodov, I. V. Kukushkin, and S. Schmult, Phys. Rev. B **95**, 161305(R) (2017).
[9] X. Fu, Q. A. Ebner, Q. Shi, M. A. Zudov, Q. Qian, J. D. Watson, and M. J. Manfra, Phys. Rev. B **95**, 235415 (2017).
[10] A. V. Shchepetilnikov, Yu. A. Nefyodov, A. A. Dremin, and I. V. Kukushkin, JETP Lett. **107**, 770 (2018).
[11] A. A. Bykov, D. R. Islamov, A. V. Goran, and A. K. Bakarov, JETP Lett. **86**, 779 (2007).
[12] C. L. Yang, M. A. Zudov, T. A. Knuuttila, R. R. Du, L. N. Pfeiffer, and K. W. West, Phys. Rev. Lett. **91**, 096803 (2003).
[13] A. A. Bykov, JETP Lett. **87**, 233 (2008).
[14] A. A. Bykov, I. V. Marchishin, A. V. Goran, and D. V. Dmitriev, Appl. Phys. Lett. **97**, 082107 (2010).
[15] S. I. Dorozhkin, A. A. Kapustin, V. Umansky, K. von Klitzing, and J. H. Smet, Phys. Rev. Lett. **117**, 176801 (2016).
[16] I. V. Andreev, V. M. Muravev, I. V. Kukushkin, S. Schmult, and W. Dietsche, Phys. Rev. B **83**, 121308(R) (2011).
[17] A. A. Zadorozhko, Yu. P. Monarkha, and D. Konstantinov, Phys. Rev. Lett. **120**, 046802 (2018).
[18] V. E. Kozlov, A. B. Van'kov, S. I. Gubarev, I. V. Kukushkin, V. V. Solovyev, J. Falson, D. Maryenko, Y. Kozuka, A. Tsukazaki, M. Kawasaki, and J. H. Smet, Phys. Rev. B **91**, 085304 (2015).
[19] V. V. Solovyev and I. V. Kukushkin, Phys. Rev. B **96**, 115131 (2017).

[20] A. B. Van'kov, B. D. Kaysin, and I. V. Kukushkin, Phys. Rev. B **96**, 235401 (2017).

[21] A. B. Van'kov, B. D. Kaysin, and I. V. Kukushkin, Phys. Rev. B **98**, 121412(R) (2018).

[22] J. Betancourt, J. J. Saavedra-Arias, J. D. Burton, Y. Ishikawa, E. Y. Tsymbal, and J. P. Velev, Phys. Rev. B **88**, 085418 (2013).

[23] V. V. Solovyev, A. B. Van'kov, I. V. Kukushkin, J. Falson, D. Zhang, D. Maryenko 4, Y. Kozuka, A. Tsukazaki, J. H. Smet, and M. Kawasaki, Appl. Phys. Lett. **106**, 082102 (2015).

[24] J. Falson and M. Kawasaki, Rep. Prog. Phys. **81**, 056501 (2018).

[25] D. F. Karcher, A. V. Shchepetilnikov, Yu. A. Nefyodov, J. Falson, I. A. Dmitriev, Y. Kozuka, D. Maryenko, A. Tsukazaki, S. I. Dorozhkin, I. V. Kukushkin, M. Kawasaki, and J. H. Smet, Phys. Rev. B **93**, 041410(R) (2016).

[26] T. Tambo, J. Falson, D. Maryenko, Y. Kozuka, A. Tsukazaki, and M. Kawasaki, J. Appl. Phys. **116**, 084310 (2014).

[27] L. W. Engel, D. Shahar, C. Kurdak, and D. C. Tsui, Phys. Rev. Lett. **71**, 2638 (1993).

[28] X. Fu, A. Riedl, M. Borisov, M. A. Zudov, J. D. Watson, G. Gardner, M. J. Manfra, K. W. Baldwin, L. N. Pfeiffer, and K. W. West, Phys. Rev. B **98**, 195403 (2018).

[29] I. V. Andreev, V. M. Muravev, V. N. Belyanin, and I. V. Kukushkin, Appl. Phys. Lett. **105**, 202106 (2014).

[30] M. Khodas and M. G. Vavilov, Phys. Rev. B **78**, 245319 (2008).

[31] M. A. Zudov, O. A. Mironov, Q. A. Ebner, P. D. Martin, Q. Shi, and D. R. Leadley, Phys. Rev. B **89**, 125401 (2014).

[32] R. Yamashiro, L. V. Abdurakhimov, A. O. Badrutdinov, Yu. P. Monarkha, and D. Konstantinov, Phys. Rev. Lett. **115**, 256802 (2015).